Environmental Pollution 359 (2024) 124596

Contents lists available at ScienceDirect

Environmental Pollution

journal homepage: www.elsevier.com/locate/envpol

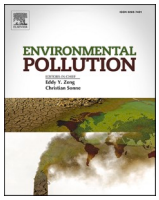

Glyphosate and other plant protection products in size-segregated urban aerosol: Occurrence and dimensional trend

Giovanna Mazzi [a], Matteo Feltracco [a,*], Elena Barbaro [b], Agata Alterio [a], Eleonora Favaro [a], Chafai Azri [c], Andrea Gambaro [a]

[a] Department of Environmental Sciences, Informatics and Statistics, Ca' Foscari University of Venice, Via Torino 155, 30172, Venezia Mestre, Italy
[b] Institute of Polar Sciences, National Research Council, Via Torino 155, 30172, Venezia Mestre, Italy
[c] Research Laboratory of Environmental Sciences and Sustainable Development "LASED", LR18ES32, University of Sfax, Sfax, Tunisia

ARTICLE INFO

Keywords:
Glyphosate
Emergent contaminants
Size-segregated urban aerosol
Ion chromatography tandem mass spectrometry

ABSTRACT

Plant protection products (PPPs) play a fundamental role in the maintenance of agricultural fields and private/public green areas, however they can contaminate zones nearby the application point due to wind drift, resuspension, and evaporation. Several studied have deepened the relationship between PPPs and living beings' health, suggesting that these products might have a negative influence. Some PPPs belong to the class of Emergent Contaminants, which are compounds whose knowledge on the environmental distribution and influence is limited. These issues are even more stressed in urban aerosol, due to the high residential density that characterizes this area. Therefore, this study assessed the contamination caused by polar PPPs, such as herbicides (i.e., Glyphosate), fungicides (i.e., Fosetyl Aluminium), and growth regulators (i.e. Maleic Hydrazide), in size-segregated urban aerosol and evaluated their concentration variability with respect to atmospheric parameters (humidity, temperature, rain). Moreover, hypotheses on possible sources were formulated, exploiting also back-trajectories of air masses. A total of six PPPs were found in the samples: glyphosate was more present in the coarse fraction (2.5–10 μm), Fosetyl Aluminium, chlorate and perchlorate were more present in the coarse/fine fractions (10-1 μm), while cyanuric acid and phosphonic acid were mostly concentrated in the fine/ultrafine fractions (<1 μm). While for the first four we suspect of local sources, such as private gardening, the two latter might derive from the entire Po Valley, a highly polluted area in the North of Italy, and from degradation of other substances.

1. Introduction

Atmosphere of urban areas is known to be strongly polluted by particulate matter (PM) especially due to anthropogenic sources such as traffic exhaust, domestic heating, worksites, and industrial emissions (Li et al., 2020). As confirmed by papers, global reports and international guidelines, PM has become a dramatic issue in recent years, being culpable of many cardiovascular and respiratory diseases, strokes and many premature deaths, and appears also to be a climate forcing agent (Chen et al., 2020; Colbeck and Lazaridis, 2010; Elser et al., 2016; Garcia et al., 2023; "WHO global air quality guidelines, 2021), although there are still some uncertainties on the overall effect on temperature. For instance, black carbon, a component of atmospheric PM, is composed of light-absorbing particles that affect climate warming but whose radiative forcing remains to be further investigated (Singh et al., 2016).

PM can be divided in three major categories, based on the aerodynamic diameter: coarse (10–2.5 μm), fine (2.5–0.1 μm) and ultrafine (<0.1 μm) particles (Colbeck and Lazaridis, 2010). Particulate size is a parameter that influences aerosols' atmospheric dynamics, deposition, transport and residence time, but it is also tightly connected to aerosol's hazard (Colbeck and Lazaridis, 2010). While particles with an aerodynamic diameter higher than 10 μm are commonly blocked outside the human organism by the nose, those with a lower diameter can enter the body. Depending on the size, the particles can reach different levels of the respiratory tract. If the diameter is lower than 2.5 μm, the particulate can penetrate in the lungs and eventually reach the alveoli. Ultimately, ultrafine particles (<0.1 μm) can enter the bloodstream (Colbeck and Lazaridis, 2010). Moreover, fine and ultrafine particles have a higher

* Corresponding author.
E-mail addresses: giovanna.mazzi@unive.it (G. Mazzi), matteo.feltracco@unive.it (M. Feltracco), elena.barbaro@cnr.it (E. Barbaro), agata.alterio@unive.it (A. Alterio), eleonora.favaro@unive.it (E. Favaro), chafaiazri@yahoo.fr (C. Azri), andrea.gambaro@unive.it (A. Gambaro).

https://doi.org/10.1016/j.envpol.2024.124596
Received 4 April 2024; Received in revised form 18 July 2024; Accepted 21 July 2024
Available online 23 July 2024

surface area compared to the coarse fraction, and are more porous, therefore are more prone to adsorb and retain substances (Coscollà et al., 2013). As such, it is important to deepen the knowledge on pollutants' distribution in the different dimensional ranges.

A key topic in environmental research are the Contaminants of Emerging Concern (CECs), defined as compounds that are known to be present in the environment but whose legislation is lacking or missing, and include also plant protection products (PPPs), pharmaceuticals and personal care products (Caixeta, 2023). They were first listed in 2015 by the European Commission within the framework of surface water pollution, and in the following years the list was updated consistently with the experimental evidences ("Surface water - European Commission, 2023). However, only a restricted amount of works focuses on CECs in atmosphere, which is a critic lack of information since air act also as a substances' vector.

PPPs cover a fundamental role in agricultural, private, and public areas, as they support plant growth (nutrients), kill unwanted weeds, reduce risk of infection, and prevent parasites attack (pesticides, insecticides, fungicides …) (Pogacean and Gavrilescu, 2009). Nevertheless, they also represent a source of pollution. Spray drift, volatilization, and wind erosion of contaminated soil are the three main pathways that can lead to atmosphere contamination, both of gaseous and particulate phase (Coscollà et al., 2013). Organochloride and organophosphorus pesticides (OCPs and OPPs, respectively) were studied in urban and rural environments: Coscollà et al. (2013) detected commonly used pesticides (CUPs) in the fine fraction of rural atmosphere in France during the period of fields treatment, with concentration ranging from 0.08 to 1.5 ng m^{-3}. In a traffic area of Thessaloniki, Chrysikou et al. (2009, 2009) studied the seasonal and vertical variation of several atmospheric pollutants and OCPs. Evidence shows that the analytes were most present in smaller particulate fractions (<0.95 μm) in winter, while in summer a small shift towards bigger particles was detected (Chrysikou et al., 2009; Chrysikou and Samara, 2009). However, to the best of our knowledge, no studies have evaluated the size-segregated distribution of glyphosate and other polar pesticides in urban aerosol. Sousa and co-workers (2019) evaluated presence of glyphosate in the total suspended particulate (TSP) in urban and rural areas in the North of Brazil (de F. Sousa et al., 2019), while another study focused on the glyphosate concentration in the PM_{10} of a rural area and in the surrounding roads (Ramirez Haberkon et al., 2021). In 2019, Ravier et al. conducted a study on glyphosate presence in different areas (urban, rural, industrial, agricultural) and detected the herbicide on PM_{10} aerosol filters (Ravier et al., 2019). PPPs were found even at 2543 m a.g.l., at the Col Margherita Observatory located in the Italian Dolomites, where the local contribution is minimal compared to the long-range transport (Feltracco et al., 2022).

Considering that plenty of studies have confirmed the toxicity of different PPPs, (DeLorenzo et al., 2001; Mostafalou and Abdollahi, 2017; Mrema et al., 2013; Sidhu et al., 2019; Singh et al., 2016) and that pesticides can be subjected to long-range transport (Feltracco et al., 2022), they might represent a tackle to human and animals' health. Acknowledged that size distribution is fundamental to assess human exposure, and that pesticide presence in the atmosphere is still an understudied field, much effort must be put in filling this knowledge gap.

For the scope of the study, a total of 13 analytes were studied: *Glyphosate* (N-(phosphonomethyl)glycine; Gly*)*, the most used broad-spectrum, non-selective herbicide introduced on the market in 1976, employed both in crop field but also in private and public gardens (Kontogiannatos et al., 2020). Two of its major by-products, (*Aminomethyl)phosphonic acid* (*AMPA*), produced by microbial breakage of the carbon-nitrogen bond in soil and water, and *N-acetyl glyphosate* (*GlyAc*) were also object of this study. *Glufosinate* (2-amino-4-(hydroxy(methyl) phosphoryl) butanoic acid; *Gluf*) is a wide-spectrum systemic agent used for weeds control, however in 2018 the approval from the European Commission has expired and it should no longer be used in agriculture (Commission Implementing Regulation (EU) 2015/408, 2015). Two of its derivatives, *N-acetyl glufosinate* (*GlufAc*) and *3-methyl-phosphinicopropionic acid* (*MPPA*), were also included in the study. *Fosetyl aluminium (Fos-Al)*, used to prevent fungal infections on grapevines, is commonly used in orchards, but it is forbidden in organic farming and in those productions whose output is processed to obtain particular products, e.g. baby food. It is regulated by the Reg. CE n. 1107/2009, concerning the placing of plant protection products on the market (Regulation (EC) No 1107/2009, 2009). *Phosphonic acid* (*PA*), both fungicide and fertilizer, is also a by-product of Fos-Al and other phosphorous fertilizer. *Ethephon* (2-chloroethylphosphonic acid; *Ete*), an organophosphorus systemic growth regulator, and its major derivative *ethephon-hydroxy* (2-hydroxyethyl)phosphonic acid, also known as *HEPA*). *Maleic hydrazide* (*Mal H*) is employed to control grape growth. *Cyanuric acid* (*CA*), a common disinfectant and sanitizer, it is used also as stabilizer to maintain the germicidal efficacy of chlorinated disinfectants in swimming pools (Chen and Su, 2024). It can also derive from thermal degradation of urea and is the major microbial by-product of melamine through hydrolyzation of the aminic group (Dorne et al., 2013; Zhu et al., 2019). It must be noted that the sampling site is close to an industrial area which includes a plant that produces melamine cyanurate (3 V Sigma), which might represent a non-negligible source of CA. Finally, the last two compounds are *chlorate* (ClO_3^-; *Chl*) and *perchlorate* (ClO_4^-; *Prc*), two disinfection byproducts often detected on food and beverages; the latter can also derive from photooxidation reaction in atmosphere of PPPs containing chlorine (Jackson et al., 2018). All the corresponding structures and abbreviations can be found in Supporting Table S2. To the best of our knowledge, this is the first time that this array of compounds is studied in size-segregated urban aerosol. As PM pollution is particularly high in urban areas, and knowledge on PPPs aerosol distribution is still a major lack to overcome, this work aims to implement knowledge on emergent contaminants' distribution in urban environment, especially in dimensional ranges, and to study possible sources willing to furnish solid data for policy makers.

2. Experimental

2.1. Materials and methods

Ultrapure water (18.2 MΩ-cm, 1 ppb TOC) was produced using a Purelab Ultra System (Elga®, High-Wycombe, UK) and ultra-grade methanol (MeOH) was purchased from VWR® (Radnor, PA, USA). Glyphosate (s), glufosinate (s), MPPA (s) and the internal standards glyphosate-2-^{13}C,^{15}N (s) and AMPA-^{13}C,^{15}N (l, 100 μg mL^{-1} in H_2O) were purchased from Merck KGaA (Darmstadt, Germany). Cyanuric acid (s), phosphonic acid (s), N-acetyl AMPA (s), ethephon (s), HEPA (s), N-acetyl glufosinate (s), maleic hydrazide (s), FOS-Al (s) and the internal standard FOS-Al ^{15}D (s) were purchased from LCG Standards (Teddington, UK). Chlorate (l, 1000 μg mL^{-1} in H_2O) and perchlorate (l, 1000 μg mL^{-1} in H_2O) were purchased from VWR Chemicals (Radnor, Pennsylvania, USA). The solid standards were diluted in ultrapure water.

For the sampling, aluminium disks (diameter 47 mm) were autoproduced by cutting commercially available aluminium foil with a die-cut, while quartz filters (diameter 47 mm, Cod. MFQ/047, MFQ Filter Lab) were purchased from Filtros Anoia (Barcelona, Spain).

For the sample treatment, 15-mL plastic tubes (Sarstedt, Nümbrecht, Germany) and an ultrasonic bath (Ceia CP104) filled with ultrapure water were employed. The extract was filtered using a 5 mL plastic syringe (Braun, Melsugen, Germany) equipped with a 0.45 μm PTFE filter (ChromaScience, Istanbul, Turkey).

3. Sampling

The sampling site is located in Mestre (Venice), a city with around 200,000 inhabitants in the Veneto region of North-East Italy (Fig. 1).

Fig. 1. Geographical location of the sampler and details of the sampling site (rooftop of Alfa building).

Mestre is a trafficked city, with several major highways surrounding it (SR11, SR14, SS14), and many medium and minor roads. In 2012 it was studied the city traffic using 14 monitoring stations and results showed that just in the temporal interval 8:15–8:30 a.m., more than 3400 vehicles crossed the roads, in both directions (SM612389, 2019).

The sampling site is particularly interesting because it is close to several busy roads (SR14, SS14), it is close to the industrial area of Porto Marghera (ca. 2.5 km), close to the Venetian Lagoon (ca. 3.0 km) and several public parks (Forte Marghera (ca. 0.5 km), San Giuliano Park (ca. 1.5 km), Osellino Park (ca. 1.0 km).

The sampler was put on the rooftop (ca. 35 m) of a building in the Scientific Campus (Via Torino 155, 30170 Mestre, Venice (VE), Italy). This location allowed us to sample aerosol coming from local short- and long-range transport, which we expect to be important as PPPs are used in larger quantities in rural sites, by avoiding any kind of shielding from higher close buildings. This, moreover, limits the contribution from resuspension due to the highness of the sampling site, which we wanted to avoid in order to and focus only on local and non-local transport. In the Supporting information are collected some pictures of the rooftop (Supporting Fig. S1).

The sampler employed is a 10-stages cascade impactor (Micro-Orifice Uniform Deposit Impactor, MOUDI, Model 110NR, MSP Corporation, Shoreview, Minnesota, USA; Supporting Fig. S2), with the following size classes: Inlet: >18 μm, Stage 1: 18 to 10 μm, Stage 2: 10 to 5.6 μm, Stage 3: 5.6 to 3.2 μm, Stage 4: 3.2 to 1.8 μm, Stage 5: 1.8 to 1.0 μm, Stage 6: 1.0 to 0.56 μm, Stage 7: 0.56 to 0.32 μm, Stage 8: 0.32 to 0.18 μm, Stage 9: 0.18 to 0.10 μm, Stage 10: 0.10 to 0.056 μm, backup filter (outlet): <0.056 μm. For every sampling, each plate stage was loaded with a 47 mm disk of aluminium foil, while the outlet that was equipped with a 47 mm quartz filter, previously pre-combusted at 400 °C for 4 h. Prior to every sampling, the MOUDI sampler and the aluminium disks were carefully washed and decontaminated with ultragrade methanol (MeOH). The aluminium disks and the quartz filter were weighted before the sampling (Pioneer PX balance, OHAUS Europe GmbH, Nänikon, Switzerland). The aspiration flow of the MOUDI is 30 L min^{-1} and it was checked before and after every sampling with a flowmeter (Model 6001/Fe, Tecfluid, Sant Just Desvern, Barcelona, Spain), together with the checking in the control module that the pressure drop across the impactor stages were coherent with the productor specifications (Supporting Fig. S2). No substantial drop (<5%) in flow rate was observed at the end of each sampling.

Samples were collected from August 1st, 2023, to October 16th, 2023, covering most of the summer and almost all the first month of autumn. The time resolution varied from seven to ten days. In Table 1 are reported some specifics of the samples and of the prevailing atmospheric conditions. After the sampling, all the samples were weighted three times, fourth-folded, transferred into a double aluminium pocket to avoid both contamination and sample loss, and finally stored at −20 °C until analysis.

Blanks were obtained by loading the sampler with decontaminated aluminium disks and quartz filter, leaving them for few minutes, and then transferring to aluminium pockets. Blanks were kept at −20 °C as the samples until analysis.

3.1. Sample treatment and instrumental analysis

For the sample preparation, both aluminium and quartz samples were transferred into a 15 mL plastic tube, next 10 μg L^{-1} of internal standards were added. Extraction was performed with 10 mL of ultrapure water for 30 min in ultrasonic bath, then the supernatant was filtered into a 1.5 mL glass vial using a plastic syringe equipped with a 0.45 μm filter. Samples were stored at −20 °C until analysis.

Analysis was performed with using a HPAEC (Dionex™, Thermo Scientific™, ICS-5000, Waltham, USA) coupled to a TSQ Altis™ Plus Triple Quadrupole Mass Spectrometer (Thermo Scientific™, USA) using an electrospray source (ESI) that operated in negative mode. Chromatographic separation was performed using an anion exchange column Dionex IonPac™ AS19 RFIC™ 2 × 250 mm (Thermo Scientific™) equipped with a guard column Dionex IonPac™ AG19 RFIC™ 2 × 50 mm (Thermo Scientific™). More details on the chromatographic

Table 1
Average atmospheric conditions of the samplings.

Period of sampling (dd/mm/yyyy)	Volume sampled (m^3)	Average atmospheric conditions				
		Temperature min-max (°C)	Rain (total mm)	Average humidity (%)	Solar radiation (W m^{-2})	Average wind speed (m s^{-1})
1-11/08/2023	426.6	11.8–30.1	19.0	80	728.1	1.4
11-21/08/2023	429.3	15.2–33.8	0.2	75	1012.0	1.0
21-31/08/2023	435.6	27.5–35.1	49.2	77	676.4	1.2
31/08–11/08/2023	469.8	13.2–30.4	0.2	74	818.3	1.2
11-18/09/2023	289.8	13.0–29.7	1.0	81	438.7	0.9
18-25/09/2023	293.4	11.0–28.8	4.6	81	446.7	1.2
25/09–2/10/2023	298.8	11.0–29.2	0	72	643.6	1.3
2-9/10/2023	297.9	9.4–26.4	0.6	76	554.5	1.0
9-16/10/2023	286.2	10.9–25.6	0.2	82	299.2	1.1

separation and on mass spectrometer's specifics can be found in Feltracco et al. (2022) and in the Supporting Table S3.

3.2. AQ/CQ validation

Extraction of the analytes from the quartz filter was previously validated by Feltracco et al. (2022). Extraction from the aluminium disks was validated within this study. For the validation, the internal standard (IS*) Fos-Al* was used to quantify Fos-Al, Chlorate, Perchlorate, Cyanuric Acid and Phosphonic Acid, while Gly* was used as internal standards to quantify Ethephon-OH, Gluf, Maleic H, NAc-AMPA, NAc-GLUF, AMPA, MPPA, ethephon and Gly. Both of the ISs were spiked at a concentration of 10 ng mL^{-1}. Blanks were obtained by ultrasonically extracting aluminium disks with 10 mL of water and the ISs. Trueness were obtained by spiking aluminium disks with 10 ng mL^{-1} of ISs and 10 ng mL^{-1} of native compounds and then extracting ultrasonically with 10 mL of ultrapure water. Validation parameters such as method detection limit (MDL) and method quantification limit (MQL) are summed in Table 2; limit of detection (LOD) and quantification (LOQ) for each analyte can be found in Feltracco et al. (2022). All the compounds showed a trueness between −9 and +10, with a reproducibility lower that 10%. Blanks were in general low, although Fos Al, Gluf, Mal-H and MPPA showed higher blanks. MDL and MQL are generally lower for aluminium compared to quartz filter reported in the validation of Feltracco et al. (2022). Validation and determination of AMPA was non performed since Feltracco et al. (2022) did not detect this compound in any of the aerosol samples collected in a rural site. Regarding Fosetyl Aluminium, it must be highlighted that it is a complex made of three Fosetyl moieties coordinated with an Aluminium(III) ion, thus the analysis quantifies only the Fosetyl moiety and not the complex.

3.3. ARPAV data

Daily and hourly atmospheric parameters (minimum. maximum and average temperature. average humidity, total rain, average wind speed, average solar radiation) were retrieved from the Veneto Regional Agency of Environmental Protection and Prevention (ARPAV) monitoring station located in Parco Bissuola (Mestre, Italy). This station is the closest (ca. 3.5 km) to the sampling site and is located 2 m high from the ground.

Table 2
MDL, MQL, trueness, precision, and blanks of the aluminium validation. MDLs and MQLs are reported as ng on the average volume of air sampled (ng m^{-3}).

Compound	MDL (ng m^{-3})	MQL (ng m^{-3})	Trueness (%)	Precision (CV%)	Blank ± dev. std. (ng)
Gly	0.000002	0.000008	−6	4	0.0040 ± 0.0003
GlyAc	0.000004	0.000013	9	4	0.0047 ± 0.0005
Gluf	0.000317	0.001058	−3	10	0.54 ± 0.04
GlufAc	0.000034	0.000112	3	8	0.081 ± 0.004
MPPA	0.000075	0.000250	−9	8	0.124 ± 0.009
Fos Al	0.000101	0.000336	−7	2	0.66 ± 0.01
PA	0.000008	0.000027	−9	5	0.015 ± 0.001
Ete	0.000019	0.000062	8	9	0.060 ± 0.002
HEPA	0.000015	0.000050	−10	7	0.020 ± 0.002
Mal- H	0.000217	0.000724	−3	10	0.28 ± 0.03
CA	0.000014	0.000045	−9	4	0.019 ± 0.002
Chl	0.000037	0.000124	3	6	0.053 ± 0.004
Prc	0.000012	0.000041	−2	8	0.027 ± 0.001

3.4. RStudio elaboration data

To elaborate data in RStudio, the library GGally was employed. To obtain the correlation matrix, it was used the GGcorr function with the specific dataset containing the atmospheric parameters retrieved by ARPAV.

3.5. HYSPLIT back-trajectories model

Air masses back trajectories were determined using the National Oceanic and Atmospheric Administration (NOAA) Hybrid Single-Particle Lagrangian Integrated Trajectory (HYSPLIT) model (Draxler and Hess, 1998). The location was set at 45.5 longitude and 12.3 latitude. The bottom of the model was set at 60 m, the top model was set at 6000 m a.g.l., and monitoring of air transport was performed till 120 h before the start of the sampling to 10 or 7 days after. Time interval was set at 6 h. The meteorological data were in the GDAS format and were retrieved from the NOAA archive directly through the HYSPLIT programme, with 1° resolution.

4. Results and discussion

4.1. PM concentration

PM concentration was calculated for each stage and each sampling (Fig. 2). The average PM_{10} concentration was around 20 μg m^{-3}, although a decisive increase in mass concentration was observed for the last two samplings, which cover the first two weeks of October (2–16/10/2023). Size-segregated concentrations of PM are reported in the Supporting Information (Table S4).

Fig. 2b displays the Total Suspended Particles (TSP), calculated by summing the PM sampled by the MOUDI of all stages, the PM_{10} (coarse fraction upper limit), the $PM_{1.8}$ (fine fraction upper limit), and $PM_{0.1}$ (ultrafine fraction upper limit) collected by the MOUDI. Since the sampler does not have a 2.5 μm cut off, it was decided to use 1.8 μm as upper limit of the fine particles. As can be seen, the increase in PM concentration is present in TSP, PM_{10} and $PM_{1.8}$, while the ultrafine particles ($PM_{0.1}$) remain almost constant during the samplings. Specifically, the major contribution to PM increase was led by an increase in particles in the range 1–0.56 μm (stage 7), as shown in Fig. 2b. As previously demonstrated (Vicente and Alves, 2018) biomass combustion-based domestic heating produces fine particles. Thus, this enhancement in the fine fraction might shows the beginning of private heating, probably coming from the Northern part of the Veneto region where biomass burning is often used as heating system (the Italian legislation sets the November 15th as the first day of centralized heating). For each of the sampling a back-trajectory was created with the NOAA Hysplit model (Figs. S5–13, Supporting Information). As displayed, for all the samplings the major contribution is provided by slow winds below 1000 m, often below 500 m, which reach the sampler by crossing Switzerland and Austria and encircling the Italian Alps. Thus, the principal contributions to the aerosol composition derive from winds that do not travel much (probability of 32–72%, Figs. S5–13, compared to the contribution of winds that come from the Atlantic Ocean and from bigger distances (probability of 3–25%, Figs. S5–13). This highlights that the atmosphere is relatively static and that there is a poor movement of the pollution. Especially the back-trajectories of the last three samplings (2–16/10/2023) support the hypothesis stated above (Supporting Figs. S11–13), indeed the probability of that air mass movement is 72%, 66% and 58%, respectively. To remember that the sampling site is in the Po Valley, a well-known polluted area of the North of Italy,

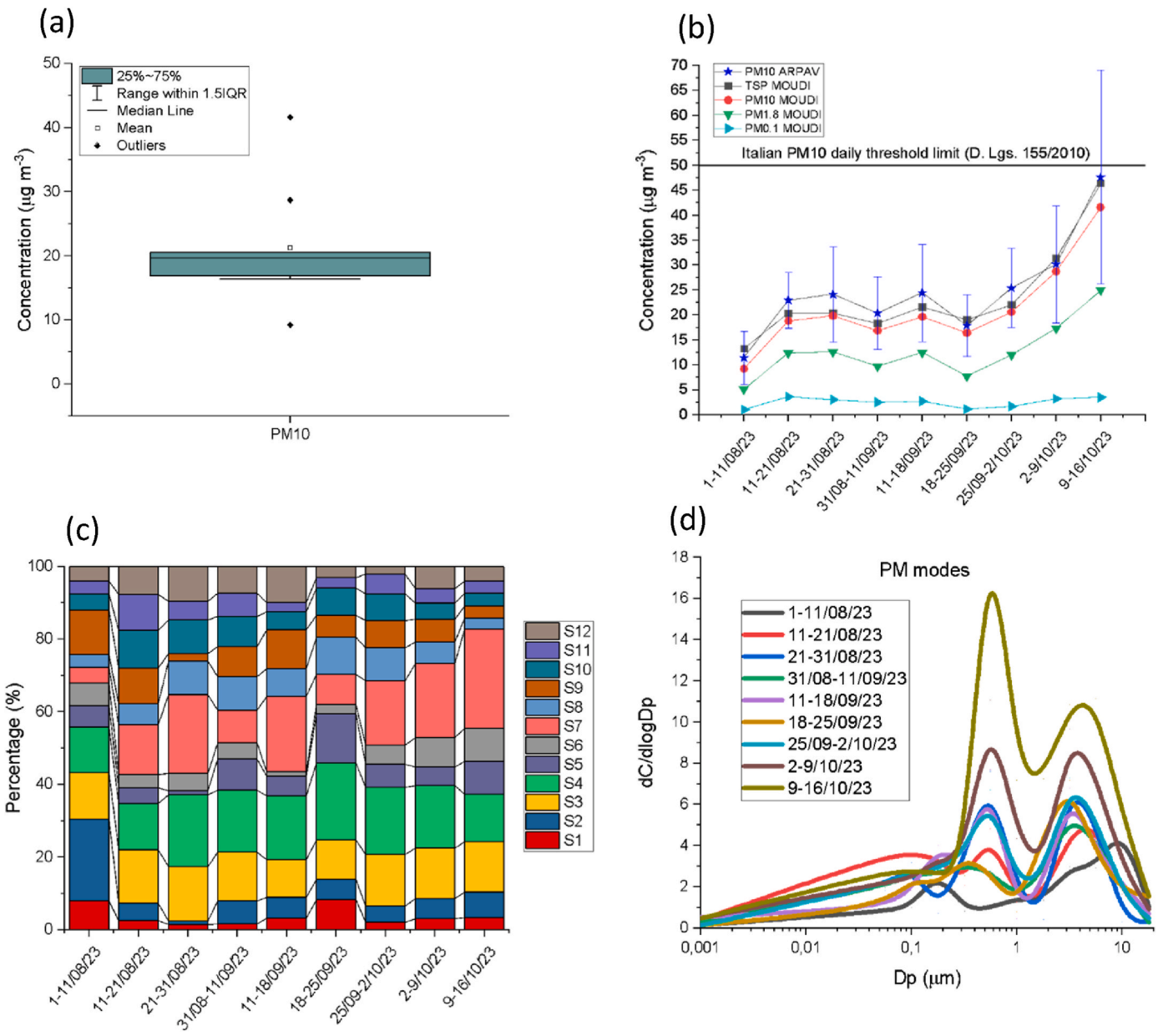

Fig. 2. Boxplot (a); TSP, Coarse (PM_{10}), fine ($PM_{1.8}$) and ultrafine ($PM_{0.1}$) temporal variability with standard deviation (b); fractions (c); and modes (d) of PM. Abbreviations can be found in Tables S1–S2 (Supporting information).

which might have acted as diffused source of PM due to the mix layer.

The higher PM_{10} concentration in the last two samplings was observed also by the Veneto Regional Agency of Environmental Protection and Prevention (ARPAV) in the closest environmental monitoring station (Parco Bissuola). The station, which measures daily PM_{10}, is located 2 m from the ground. In Fig. 2b is reported the average PM_{10} concentration collected during the same sampling period of the MOUDI sampling campaign. The trend displayed by the two sampling sites is similar, which might suggest that are affected by the same sources.

PM modes show a bimodal size distribution (Fig. 2d), as already reported in previous studies (Chrysikou and Samara, 2009; Manojkumar and Srimuruganandam, 2021). The two maxima lie around 0.6 µm (fine) and 4 µm (coarse). The former can be reconducted to traffic emissions and domestic heating, while the latter can derive by the sea salt marine aerosol, as the sampling site is close to the Venetian Lagoon (Barbaro et al., 2019; Gantt and Meskhidze, 2013; Heintzenberg et al., 2000); resuspension phenomenon might have also contributed to the coarse fractions (Chrysikou and Samara, 2009), but limitedly due to the height of the sampling site. To notice that the first three samplings (1–31/08/2023) display presence of a third maxima in the ultrafine region (0.1 µm). These are the sampling covering the month of August, which is characterized by an intense solar radiation that might have increased ultrafine particles formation through gas-to-particle conversion driven by photochemical processes (Zilli Vieira and Koutrakis, 2021).

4.2. Pesticides concentrations

Among all the compounds analysed, six of the 14 analytes were above the quantification limits and could be quantified. Results are collected in Fig. 3, where there are reported both the modes and the concentration variability of the six analytes, and in Fig. S3 which displays the average TSP concentration for each quantified analyte. It is possible to notice that Glyphosate is more present in the coarse fractions (>18–1.8 µm, stages 1–5), and in minor importance in the fine (1.8–0.32 µm, stage 6–7), Fos-Aluminium, Chlorate and Perchlorate are

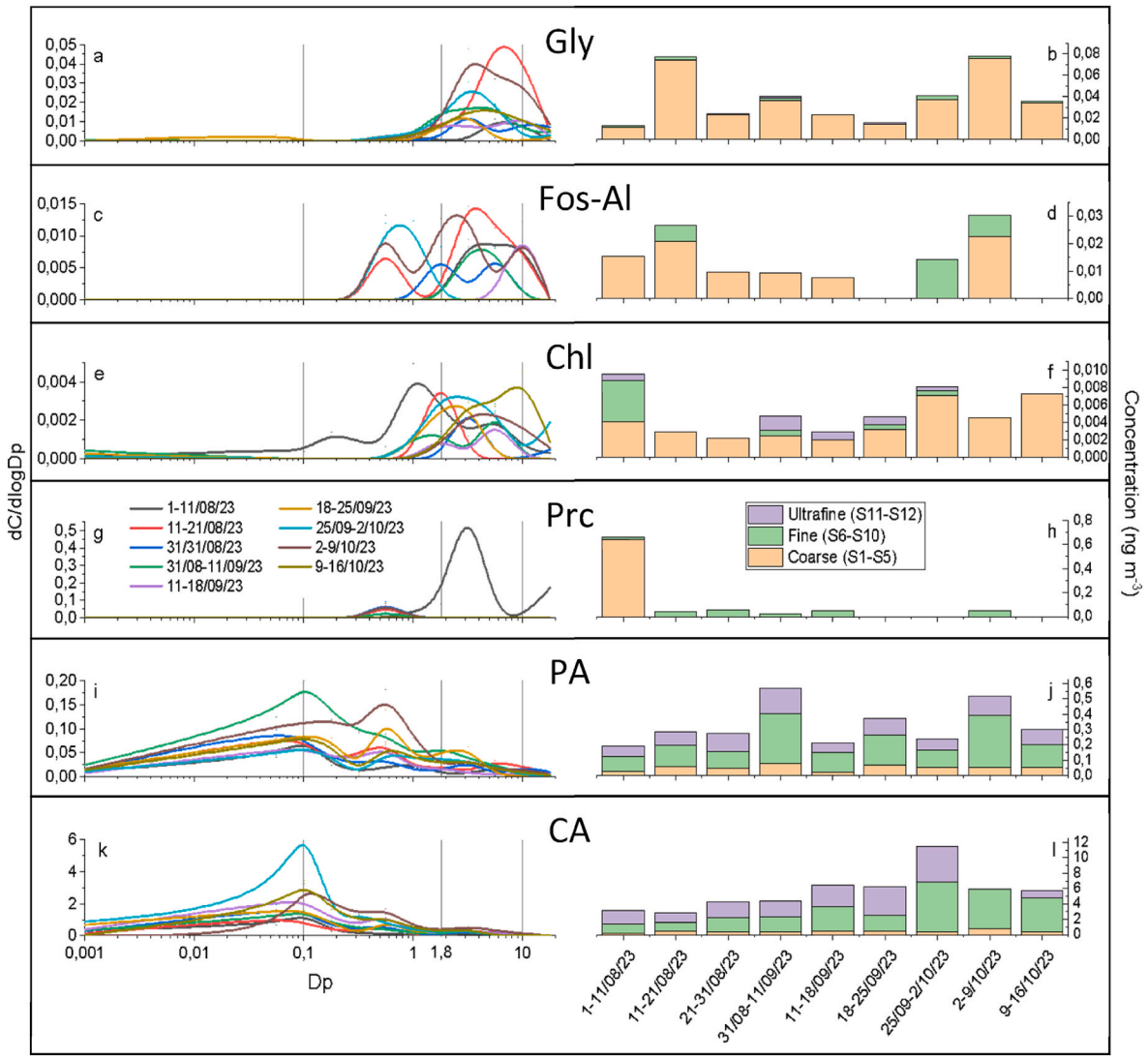

Fig. 3. Graphics on the left represent the modes of the six analytes, while the graphics on the right report the temporal size-segregated concentration of the same compounds. Abbreviations can be found in Tables S1–S2 (Supporting information).

spread around coarse and fine, while Cyanuric acid and Phosphonic acid are more concentrated in the fine (1–0.1 μm, stages 6–9) and ultrafine (0.1-<0.056, stages 10–12) fractions. As such, the two latter should be more influenced by long-range transport as smaller particles are moved more easily than coarse fractions. Contrary to what was previously found in rural and mountainous sites (Feltracco et al., 2022), HEPA was never detected. The sampling periods of the two works are compatible, as both are focused on the summer-fall period, thus it is less likely that the absence of HEPA is due to a different timing of field treatment. Rather, this difference suggests that sources of the parent compound, Ete, are located far from the sampler used in this study, and that even if Ete was photoxidized into HEPA, it does not reach the sampling area.

Glyphosate (Fig. 3a and b) shows a monomodal size distribution with a peak centred between 3 and 7 μm for almost all the samplings. The highest concentration reached in the TSP was 0.08 ng m^{-3}, while it reached 0.05 ng m^{-3} in PM10. One of our previous article dealt with the presence of pesticides in rural and mountain PM_{10} aerosols (Feltracco et al., 2022). The highest registered concentration of glyphosate was 0.45 ng m^{-3} for the former environment and 0.03 ng m^{-3} for the latter. It appears that urban samples are much less polluted than the agricultural areas, compared also to other findings (de F. Sousa et al., 2019; Ravier et al., 2019). Glyphosate microbial by-product (AMPA) was never detected, which is a common finding. Indeed, Ravier and coworkers (2019) hypnotized that the major source of glyphosate in atmosphere is the drift phenomenon during its application, instead of polluted soil resuspension, which could lead to formation various glyphosate metabolites. Since the tendency to drift of a particle is related to its dimension and since this study has proven that glyphosate is more present in the coarser fractions, it might suggest that the source is local like private gardens and public green areas. Its concentration variability does not show a clean pattern, suggesting that either glyphosate presence in the aerosol is not connected to one single source or that its usage is not linked to cyclic treatments but more to independent, random applications.

Fos-Al (Fig. 3c,d), a fungicide used in orchards and grapewines, displays monomodal, bimodal and trimodal size distribution across coarse and fine fractions, and it reaches the maximum (0.03 ng m^{-3} for the TSP, 0.02 ng m^{-3} for the PM_{10}) in the second-to-last sampling period. Previously, Feltracco et al. (2022) found 0.99 ng m^{-3} in rural PM_{10} aerosol, while in the mountain aerosol it was negligible. Fos-Al is not a stable compound and metabolise easily into fosetyl after application, which degrades further into phosphonic acid (Gormez et al., 2021). Taking also into account that Fos-Al has a low vapour pressure (FAO, 2013), and thus it is unlikely that, once deposited on field, it passes into the atmosphere through evaporation, it might explain the low concentration detected in urban areas compared to a rural area (Feltracco et al.,

2022), together with the major distance from the source. This is supported also by the very low concentrations of Fos Al found in the remote site (Col Margherita (Feltracco et al., 2022),). As such, it is possible to conclude that the main phenomenon that influences Fos-Al concentration into the atmosphere is not the evaporation after the treatment, but the drift during orchard treatment.

Chlorate modes are centred on the fine-coarse boundary, but concentration is negligible (Fig. 3-e,f) and difficult to interpret.

Beside the first sampling (1–11/08/2023), which shows a notable concentration of perchlorate (0.66 μg m^{-3}), distributed in four size ranges (Fig. 3-g,h), Prc was found only in few samples and mostly in the fine fraction. Prc can be naturally present in the environment (Jackson et al., 2006), nevertheless the presence in the fine fraction suggests that the source might be connected to photochemical oxidation of chloride Cl^- (or Cl containing compounds) with O_3 in the atmosphere (Feltracco et al., 2022).

Regarding one of Fos Al by-product, Phosphonic acid (Fig. 3i and j) shows a variable concentration as well as its precursor, nevertheless 1) concentrations are one or two order of magnitude higher and 2) the maxima lay around the fine and ultrafine regions. This latter evidence suggests that the source is located far from Mestre city. Ph acid can be used directly as PPP, but, as mentioned above, it can also derive from the degradation of other fungicidal plant protectors – a possible pathway would be the degradation in atmosphere of the drifted Fos-Al – as well as from the earlier usage of plant strengtheners that contained phosphonic acid salts (Gormez et al., 2021). Another possible explanation for PA occurrence in fine/ultrafine fraction might be a gas-to-particle conversion. The oxidation of PH_3 gas by OH radicals forms phosphoric acid (H_3PO_4) under photochemical effect, which might then interact with other components of the atmosphere to form PA and undergo a gas-to-particle process. PH_3 gas naturally derives from soils and sediments, but can also originate from anthropogenic sources since it is used as pesticides and in the plastic additives industry (Elm et al., 2017; Lyubimov and Garry, 2010). This process is similar to what happens during the oxidation cycle that leads to sulphuric acid (Elm et al., 2017), although to our knowledge there are no solid proves of this phenomenon.

Stadt (1893) demonstrated that PA could be formed in neat (no solvent) with oxygen, under luminous phenomenon, which might support the hypothesis above. Further studies are necessary to fill the knowledge gap.

Ultimately, cyanuric acid (CA) shows a spread, bimodal distribution in most of the samplings (Fig. 3k and l), with a peak prevalence around 0.1 μm. This evidence highlights that CA is prone to long-range transport, which is in accordance with previous results (Feltracco et al., 2022) that detected its presence at high concentrations (almost 1.2 ng m^{-3}) even in PM10 of remote sites (2543 m a.s.l.). CA was the most concentrated aerosol pesticide in urban TSP, reaching 4.55 ng m^{-3} in the fraction 0.18–0.10 μm. Its concentration increases steadily until the beginning of October, when it starts to decrease. This might be reconducted either to a lower application of the substance and also to a lower thermal degradation of urea. As mentioned in the introduction, in the surrounding of sampling site is located a melamine cyanurate-based flame retardants plant production, which surely contributes to the elevated concentration of this compound in the aerosol, although it is not expected to be the major contributor as CA is preferably found in the fine/ultrafine fractions. Moreover, as reported by the ECHA website, cyanuric acid is used also as water and sewage treatment chemical and as plastic additive, therefore it is expected to be strongly present in the environment, especially if close to industrial areas.

Regarding the concentration variability, from the evidence collected (Fig. 4) it is possible to notice that, as opposite to what expected, concentrations remain almost stable when entering the autumn season (Fig. 4), which might suggest that at least glyphosate and Fos Al are still used locally in these months. On the other hand, the increase in PM concentration is not followed by an increase in PPPs concentration, which supports the hypothesis of the private heating as the cause of the PM strong increase.

The Pearson's correlation matrix for each analyte (Fos Al, Gly, CA, PA, Prc and Chl) and atmospheric parameter (minimum, maximum and average temperature, average humidity, total rain, solar radiation, average wind speed and direction) was calculated using the library

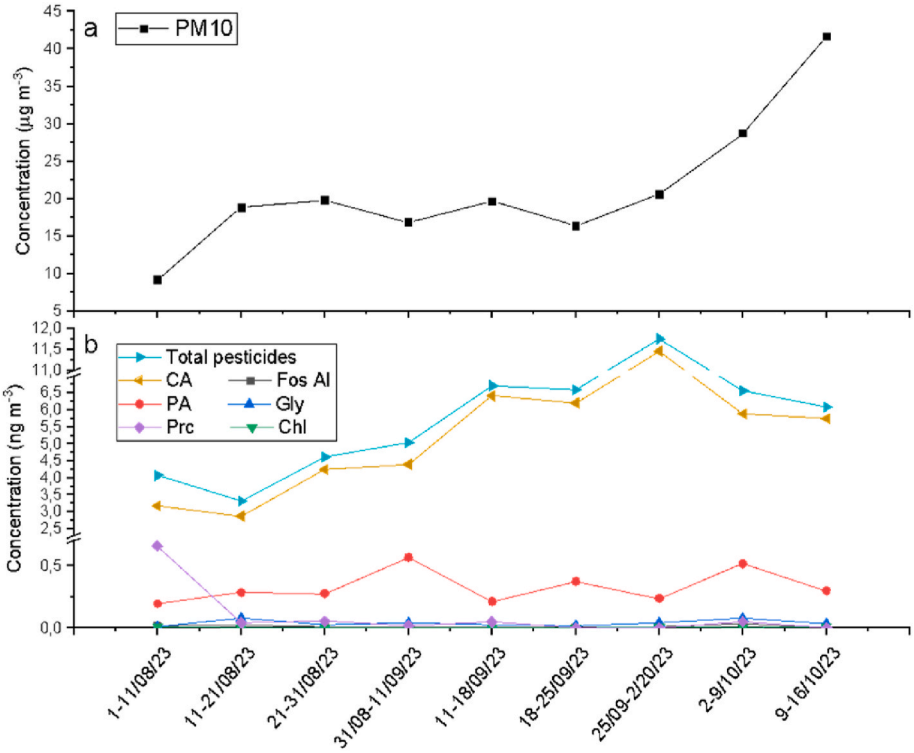

Fig. 4. Total pesticides and PM concentrations. Abbreviations can be found in Tables S1–S2 (Supporting information).

GGally and the function ggcorr() in RStudio, and it is displayed in Fig. 5. Interestingly, a positive correlation between the total trend of Fos Al and the total trend of Gly was observed, although the p-value was not significant. A possible explanation is that green areas might undergo a simultaneous treatment with the two active ingredients to prevent both weed and fungal infestation. A discrete correlation ($R^2 = 0.44$) was found between Gly and PA. A negligible correlation ($R^2 = 0.2$) between Fos Al and PA, which might support the hypothesis that degradation of Fos Al in atmosphere contributes to the presence of Ph in the aerosol, but only in small part, and thus that there are other sources that must be identified, such as the degradation of other P-based pesticides and the gas-to-particle reaction from PH_3. It is visible a discrete negative correlation also between average humidity and Fos Al. This might suggest that it undergoes scavenging, given its water solubility, which can be another issue that limits the presence of the fungicide in air. A good positive correlation ($R^2 = 0.66$) is visible among Gly and the PM. Apart from these, the other correlations are in the range $R^2 = \pm 0.40$ and can be neglected.

5. Conclusions

This study evaluated, for the first time, the occurrence of Glyphosate, Fosetyl Aluminium and several other Plant Protection Products (PPPs) in 10 dimensional classes of urban aerosol sampled at 35 m from the ground during summer and fall 2023. The remarkable results showed the presence of six compounds: Gly, Fos Al, Chl, and Prc were found mostly in the coarse/fine intervals, while PA and CA were more concentrated in the fine and ultrafine fractions. As finer fractions are more prone to travel longer distances, it is possible to assume that CA and PA come from sources located far from the sampling point, while the other four compounds might show different modes due to the use in private gardens and/or public areas located near the sampling spot. Back-trajectories of the air masses showed that the major contribution derives from slow, local winds. CA was the most concentrated compound, probably due to the many sources that contribute to its presence in the environment like thermal degradation of urea and biological degradation of melamine, together with the presence of a production

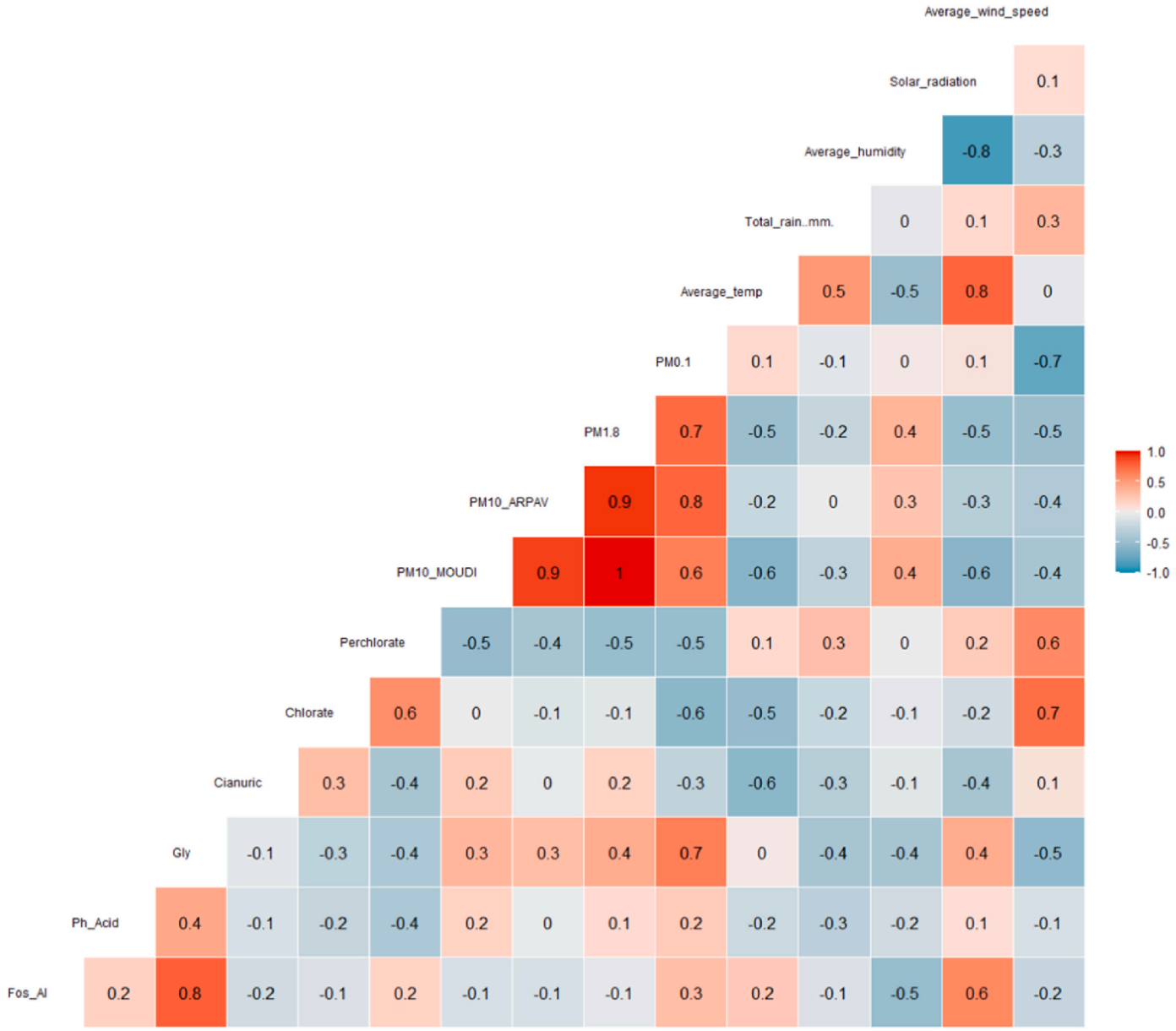

Fig. 5. Pearson's correlation matrix for analytes concentration (ng m^{-3}), PM (μg m^{-3}), temperature (°C), humidity (RH%), rain (total mm), solar radiation (W/m^2), and wind speed (m/s). The number represents Pearson's correlation coefficient.

plant close to the city. PA showed a variable concentration, which can be explained by the several sources that can cause its presence in the environment, such as Fos Al degradation and gas-to-particle reactions.

Overall, presence of PPPs in urban aerosol should rise a bell toward this kind of compounds and stimulate the scientific community to include these analytes in future works. Further insight must be done to evaluate PPPs behaviour during the other seasons, potentially focusing also on other PPPs by-products. We believe that understanding their distribution might be helpful to highlight the possible citizens' exposure and to improve policies.

CRediT authorship contribution statement

Giovanna Mazzi: Writing – original draft, Validation, Methodology, Investigation, Conceptualization. **Matteo Feltracco:** Supervision, Methodology, Conceptualization. **Elena Barbaro:** Supervision, Methodology, Conceptualization. **Agata Alterio:** Investigation. **Eleonora Favaro:** Investigation. **Chafai Azri:** Supervision. **Andrea Gambaro:** Supervision, Resources, Conceptualization.

Declaration of competing interest

The authors declare that they have no known competing financial interests or personal relationships that could have appeared to influence the work reported in this paper.

Data availability

Data will be made available on request.

Acknowledgments

The authors thank Elga Lab water, High Wycombe UK for supplying the pure water systems used in this study. The authors kindly thank ARPAV for furnishing the atmospheric data and the PM10 concentration. This article was developed within the project funded by Next Generation EU - "GRINS - Growing Resilient, INclusive and Sustainable" project (PE0000018), National Recovery and Resilience Plan (NRRP) – PE9 - Mission 4, C2, Intervention 1.3". The views and opinions expressed are only those of the authors and do not necessarily reflect those of the European Union or the European Commission. Neither the European Union nor the European Commission can be held responsible for them. This study was funded by the European Union - NextGenerationEU, in the framework of the iNEST - Interconnected Nord-Est Innovation Ecosystem (iNEST ECS_00000043 – CUP H43C22000540006). The views and opinions expressed are solely those of the authors and do not necessarily reflect those of the European Union, nor can the European Union be held responsible for them.

Appendix A. Supplementary data

Supplementary data to this article can be found online at https://doi.org/10.1016/j.envpol.2024.124596.

References

Barbaro, E., Feltracco, M., Cesari, D., Padoan, S., Zangrando, R., Contini, D., Barbante, C., Gambaro, A., 2019. Characterization of the water soluble fraction in ultrafine, fine, and coarse atmospheric aerosol. Sci. Total Environ. 658, 1423–1439. https://doi.org/10.1016/j.scitotenv.2018.12.298.

Caixeta, M.P., 2023. Contaminants of emerging concern: a review of risk assessment and treatment strategies. U.Porto Journal of Engineering 9, 191–228. https://doi.org/10.24840/2183-6493_009-001_001282.

Chen, R., Yin, H., Cole, I.S., Shen, S., Zhou, X., Wang, Y., Tang, S., 2020. Exposure, assessment and health hazards of particulate matter in metal additive manufacturing: a review. Chemosphere 259, 127452. https://doi.org/10.1016/j.chemosphere.2020.127452.

Chen, Z., Su, Y., 2024. Study on the health risk of cyanuric acid in swimming pool water and its prevention and control measures. Front. Public Health 11. https://doi.org/10.3389/fpubh.2023.1294842.

Chrysikou, L.P., Gemenetzis, P.G., Samara, C.A., 2009. Wintertime size distribution of polycyclic aromatic hydrocarbons (PAHs), polychlorinated biphenyls (PCBs) and organochlorine pesticides (OCPs) in the urban environment: street- vs rooftop-level measurements. Atmos. Environ. 43, 290–300. https://doi.org/10.1016/j.atmosenv.2008.09.048.

Chrysikou, L.P., Samara, C.A., 2009. Seasonal variation of the size distribution of urban particulate matter and associated organic pollutants in the ambient air. Atmos. Environ. 43, 4557–4569. https://doi.org/10.1016/j.atmosenv.2009.06.033.

Colbeck, I., Lazaridis, M., 2010. Aerosols and environmental pollution. Naturwissenschaften 97, 117–131. https://doi.org/10.1007/s00114-009-0594-x.

EU, 2015. Commission Implementing Regulation (EU) 2015/408 of 11 March 2015 on implementing Article 80(7) of Regulation (EC) No 1107/2009 of the European Parliament and of the Council concerning the placing of plant protection products on the market and establishing a list of candidates for substitution Text with EEA relevance. Orkesterjournalen L.

Coscollà, C., Yahyaoui, A., Colin, P., Robin, C., Martinon, L., Val, S., Baeza-Squiban, A., Mellouki, A., Yusà, V., 2013. Particle size distributions of currently used pesticides in a rural atmosphere of France. Atmos. Environ. 81, 32–38. https://doi.org/10.1016/j.atmosenv.2013.08.057.

de, F., Sousa, M.G., da Silva, A.C., dos Santos Araújo, R., Rigotto, R.M., 2019. Evaluation of the atmospheric contamination level for the use of herbicide glyphosate in the northeast region of Brazil. Environ. Monit. Assess. 191, 604. https://doi.org/10.1007/s10661-019-7764-x.

DeLorenzo, M.E., Scott, G.I., Ross, P.E., 2001. Toxicity of pesticides to aquatic microorganisms: a review. Environ. Toxicol. Chem. 20, 84–98. https://doi.org/10.1002/etc.5620200108.

Dorne, J.L., Doerge, D.R., Vandenbroeck, M., Fink-Gremmels, J., Mennes, W., Knutsen, H.K., Vernazza, F., Castle, L., Edler, L., Benford, D., 2013. Recent advances in the risk assessment of melamine and cyanuric acid in animal feed. Toxicology and Applied Pharmacology, Risk assessment of undesirable substances in feed 270, 218–229. https://doi.org/10.1016/j.taap.2012.01.012.

Elm, J., Myllys, N., Kurtén, T., 2017. Phosphoric acid – a potentially elusive participant in atmospheric new particle formation. Mol. Phys. 115, 2168–2179. https://doi.org/10.1080/00268976.2016.1262558.

Elser, M., Bozzetti, C., El-Haddad, I., Maasikmets, M., Teinemaa, E., Richter, R., Wolf, R., Slowik, J.G., Baltensperger, U., Prévôt, A.S.H., 2016. Urban increments of gaseous and aerosol pollutants and their sources using mobile aerosol mass spectrometry measurements. Atmos. Chem. Phys. 16, 7117–7134. https://doi.org/10.5194/acp-16-7117-2016.

FAO, 2013, (n.d).

Feltracco, M., Barbaro, E., Maule, F., Bortolini, M., Gabrieli, J., De Blasi, F., Cairns, W.R. L., Dallo, F., Zangrando, R., Barbante, C., Gambaro, A., 2022. Airborne polar pesticides in rural and mountain sites of North-Eastern Italy: an emerging air quality issue. Environ. Pollut. 308, 119657 https://doi.org/10.1016/j.envpol.2022.119657.

Gantt, B., Meskhidze, N., 2013. The physical and chemical characteristics of marine primary organic aerosol: a review. Atmos. Chem. Phys. 13, 3979–3996. https://doi.org/10.5194/acp-13-3979-2013.

Garcia, A., Santa-Helena, E., De Falco, A., De Paula Ribeiro, J., Gioda, A., Gioda, C.R., 2023. Toxicological effects of fine particulate matter (PM2.5): health risks and associated systemic injuries—systematic review. Water Air Soil Pollut. 234, 346. https://doi.org/10.1007/s11270-023-06278-9.

Gormez, E., Golge, O., Kabak, B., 2021. Quantification of fosetyl-aluminium/phosphonic acid and other highly polar residues in pomegranates using Quick Polar Pesticides method involving liquid chromatography-tandem mass spectrometry measurement. J. Chromatogr. A 1642, 462038. https://doi.org/10.1016/j.chroma.2021.462038.

Heintzenberg, J., Covert, D.C., Dingenen, R.V., 2000. Size distribution and chemical composition of marine aerosols: a compilation and review. Tellus B 52, 1104–1122. https://doi.org/10.3402/tellusb.v52i4.17090.

Jackson, W.A., Anderson, T., Harvey, G., Orris, G., Rajagopalan, S., Kang, N., 2006. Occurrence and formation of non-anthropogenic perchlorate. In: Gu, B., Coates, J.D. (Eds.), Perchlorate: Environmental Occurrence, Interactions and Treatment. Springer US, Boston, MA, pp. 49–69. https://doi.org/10.1007/0-387-31113-0_3.

Jackson, W.A., Wang, S., Rao, B., Anderson, T., Estrada, N.L., 2018. Heterogeneous production of perchlorate and chlorate by ozone oxidation of chloride: implications on the source of (Per)Chlorate in the solar system. ACS Earth Space Chem. 2, 87–94. https://doi.org/10.1021/acsearthspacechem.7b00087.

Kontogiannatos, D., Kourti, A., Mendes, K.F., 2020. Pests, Weeds and Diseases in Agricultural Crop and Animal Husbandry Production. BoD – Books on Demand.

Li, H., Sodoudi, S., Liu, J., Tao, W., 2020. Temporal variation of urban aerosol pollution island and its relationship with urban heat island. Atmos. Res. 241, 104957 https://doi.org/10.1016/j.atmosres.2020.104957.

Lyubimov, A.V., Garry, V.F., 2010. Chapter 104 - phosphine. In: Krieger, R. (Ed.), Hayes' Handbook of Pesticide Toxicology, third ed. Academic Press, New York, pp. 2259–2266. https://doi.org/10.1016/B978-0-12-374367-1.00104-X.

Manojkumar, N., Srimuruganandam, B., 2021. Size-segregated particulate matter and health effects in air pollution in India: a review. Environ. Chem. Lett. 19, 3837–3858. https://doi.org/10.1007/s10311-021-01277-w.

Mostafalou, S., Abdollahi, M., 2017. Pesticides: an update of human exposure and toxicity. Arch. Toxicol. 91, 549–599. https://doi.org/10.1007/s00204-016-1849-x.

Mrema, E.J., Rubino, F.M., Brambilla, G., Moretto, A., Tsatsakis, A.M., Colosio, C., 2013. Persistent organochlorinated pesticides and mechanisms of their toxicity. Toxicology, Emerging health issues from chronic pesticide exposure: innovative

methodologies and effects on molecular cell and tissue level 307, 74–88. https://doi.org/10.1016/j.tox.2012.11.015.
Pogacean, M., Gavrilescu, M., 2009. Plant protection products and their sustainable and environmentally friendly use. Environmental Engineering and Management Journal 8, 607–627. https://doi.org/10.30638/eemj.2009.084.
Ramirez Haberkon, N.B., Aparicio, V.C., Mendez, M.J., 2021. First evidence of glyphosate and aminomethylphosphonic acid (AMPA) in the respirable dust (PM10) emitted from unpaved rural roads of Argentina. Sci. Total Environ. 773, 145055 https://doi.org/10.1016/j.scitotenv.2021.145055.
Ravier, S., Désert, M., Gille, G., Armengaud, A., Wortham, H., Quivet, E., 2019. Monitoring of glyphosate, glufosinate-ammonium, and (Aminomethyl)phosphonic acid in ambient air of provence-alpes-côte-d'Azur region, France. Atmos. Environ. 204, 102–109. https://doi.org/10.1016/j.atmosenv.2019.02.023.
Regulation (EC) No 1107/2009, 2009.
Sidhu, G.K., Singh, S., Kumar, V., Dhanjal, D.S., Datta, S., Singh, J., 2019. Toxicity, monitoring and biodegradation of organophosphate pesticides: a review. Crit. Rev. Environ. Sci. Technol. 49, 1135–1187. https://doi.org/10.1080/10643389.2019.1565554.
Singh, Z., Kaur, J., Kaur, R., Hundal, S., Singh, S., 2016. Toxic effects of organochlorine pesticides: a review (open access). American Journal of Biosciences 4, 11–18. https://doi.org/10.11648/j.ajbio.s.2016040301.13.
SM612389, 2019. PUT Piano Urbano del Traffico [WWW Document]. Comune di Venezia. URL. https://www.comune.venezia.it/it/content/pgtu-piano-generale-traffico-urbano-stato-attuazione-e-aggiornamento, 4.2.24.
Surface water - European Commission, 2023 [WWW Document]. https://environment.ec.europa.eu/topics/water/surface-water_en, 1.3.24.
Vicente, E.D., Alves, C.A., 2018. An overview of particulate emissions from residential biomass combustion. Atmos. Res. 199, 159–185. https://doi.org/10.1016/j.atmosres.2017.08.027.
WHO global air quality guidelines, 2021 [WWW Document]. https://www.who.int/publications-detail-redirect/9789240034228, 1.2.24.
Zhu, H., Wang, Y., Sun, H., Kannan, K., 2019. Fertilizers as a source of melamine and cyanuric acid in soils: a nationwide survey in China. Environ. Sci. Technol. Lett. 6, 55–61. https://doi.org/10.1021/acs.estlett.8b00711.
Zilli Vieira, C.L., Koutrakis, P., 2021. The impact of solar activity on ambient ultrafine particle concentrations: an analysis based on 19-year measurements in Boston, USA. Environ. Res. 201, 111532 https://doi.org/10.1016/j.envres.2021.111532.